Diffusion-driven phase separation of deeply quenched mixtures

Natalia Vladimirova,[1] Andrea Malagoli,[2] and Roberto Mauri[1]
[1]*Department of Chemical Engineering, The City College of CUNY, New York, New York 10031*
[2]*Department of Astronomy and Astrophysics, University of Chicago, Chicago, Illinois 60637*
(Received 23 April 1997; revised manuscript received 14 September 1998)

In this work, we study the phase separation of deeply quenched mixtures in which the diffusion coefficient depends on the local composition field ϕ. In one dimension (1D), the system evolves until it reaches a spatially periodic steady state, with a period that, for instant quenching, coincides with the wavelength of the mode of maximum growth of the linear stability analysis. Similar results are obtained also when the temperature of the system is the solution of the heat equation, but in this case the period of the periodic steady-state solution increases as the heat diffusivity decreases. In 2D the concentration profile, after reaching a periodic configuration similar to the 1D steady state, continues to evolve, forming single-phase domains separated by sharp interfaces, which then thicken as the system tries to minimize its interfacial area. When the quench takes place across, or near, the critical point, the drops merge to form filaments which later coarsen and grow. However, when the quench takes place far from the critical point and near the metastable region of the phase diagram, the length of these filaments decreases as the system becomes a collection of nucleating drops. The composition field within and without these microdomains appears to be nonuniform and time-dependent even after the formation of sharp interfaces, thereby contradicting the commonly accepted assumption of local equilibrium at the late stage of the phase separation process. These results do not depend on the amount and the form of the random noise, while they are strongly influenced by the conditions of the system at the boundaries, as the morphology of phase separation becomes anisotropic and acquires a preferential direction when these conditions are not uniform. [S1063-651X(98)14212-5]

PACS number(s): 64.70.Ja, 64.60.Cn, 64.60.Ht

I. INTRODUCTION

Phase separation of deeply quenched mixtures is a problem of longstanding complexity. It can occur either by nucleation (both heterogeneous and homogeneous) or by spinodal decomposition [1]. The former process describes the relaxation to equilibrium of a metastable system, while the second one is typical of unstable systems. Therefore, nucleation is an activated process, where a free energy barrier has to be overcome in order to form embryos of a critical size, beyond which the new phase grows spontaneously; in most practical cases, suspended impurities or imperfectly wetted surfaces provide the interface on which the growth of the new phase is initiated [2].

Contrary to nucleation, spinodal decomposition occurs spontaneously, without any energy barrier to be overcome, and involves the growth of fluctuations of any amplitude that exceed a critical wavelength [3]. The classical theoretical basis of this process is the Cahn-Hilliard-Cook theory [4], generalizing the previous approach by Van der Waals [5], which was later extended to include nonlinear effects [6,7]. In principle, nucleation and spinodal decomposition are fundamentally different from each other, as metastable systems relax via the activated growth of localized fluctuations of large amplitude, whereas unstable systems do so via spontaneous growth of long-wavelength fluctuations of any amplitude. However, in practice, the distinction between the two processes is rather murky [8], as both the critical nucleus size and the critical fluctuation wavelength decrease as the temperature quench increases [9].

Experimental studies on spinodal decomposition have shown that at the end of an initial, very fast (i.e., a few milliseconds) separation process, small microdomains appear, which later grow by diffusion and coalescence [10,11]. In a recent theoretical work [12], this process of drop formation was described, generalizing the Cahn-Hilliard-Cook model using a Flory-Huggins free-energy density, with a composition-dependent diffusivity. It was found that in 1D the nonlinear terms saturate the exponential growth predicted by the linear theory, so that the concentration distribution tends to a steady-state, periodic profile, with a wavelength corresponding to the fastest growing mode of the linear regime. In addition, this steady-state profile does not depend on the form of the initial perturbation to the homogeneous composition profile.

In the present work, we intend to generalize the analysis of [12], studying a 2D system and the effects of a nonuniform, continuous quenching. In particular, we intend to compare our results with those obtained by Koch *et al.* [7] and Rogers *et al.* [13]. After briefly describing, in Sec. II, the theoretical basis of our work, in Sec. III the equations of motion are derived. Finally, after describing in Sec. IV the results of our simulation, Sec. V is devoted to a few comments and conclusions.

II. THE GOVERNING EQUATIONS

In this section we will determine the governing equation, explaining that our assumption of a composition-dependent diffusivity can be derived as a natural extension of some well-known previous works on spinodal decomposition.

Our starting point consists of a simplified dynamical model of a binary alloy, which is called model *B* in critical dynamics [14], in which the time evolution of the conserved

order parameter (i.e., the concentration of one of the constituents, in our case) is obtained by minimizing the ''coarse-grained'' free-energy functional.

A. Gibbs free energy and chemical potential

Consider a homogeneous mixture of two species A and B with molar fractions x_A and $x_B=1-x_A$, respectively, contained in a closed system at temperature T and pressure P. The equilibrium state of this system is such that it minimizes the ''coarse-grained'' free-energy functional, that is, the molar Gibbs energy of mixing, $\Delta g_{\rm eq}$,

$$\Delta g_{\rm eq}=g_{\rm eq}-(g_A x_A+g_B x_B), \tag{1}$$

where $g_{\rm eq}$ is the energy of the mixture at equilibrium, while g_A and g_B are the molar free energy of pure species A and B, respectively, at temperature T and pressure P. In turn, $\Delta g_{\rm eq}$ is the sum of an ideal part $\Delta g_{\rm id}$ and a so-called excess part $g_{\rm ex}$, with

$$\Delta g_{\rm id}=RT[x_A \ln x_A+x_B \ln x_B], \tag{2}$$

where R is the gas constant, while the excess molar free energy can be expressed as

$$g_{\rm ex}=RT\Psi x_A x_B, \tag{3}$$

where Ψ is a function of T and P. This expression, which is generally referred to as the Margules correlation [15], is generally derived by considering either the molecular interactions between nearest neighbors [16] or summing all pairwise interactions throughout the whole system [17]. In addition, as shown in the appendix of [12], Eq. (3) can be derived from first principles assuming that the $A-A$ and the $B-B$ intermolecular forces are equal to each other, i.e., $F_{AA}=F_{BB}$, so that the $g-x_A$ phase diagram is symmetric, with Ψ dependent on $(F_{AA}-F_{AB})$. In the following, we shall assume that P is fixed, so that the physical state of the mixture at equilibrium depends only on T and x_A.

Finally, in order to take into account the effects of spatial inhomogeneities, Cahn and Hilliard [4] applied an original idea by van der Waals [5] and introduced the generalized specific free energy g as

$$g=g_{\rm eq}-\frac{1}{2}RTa^2(\nabla x_A)(\nabla x_B), \tag{4}$$

where a is a typical length of the spatial inhomogeneities in the composition field. As shown by van der Waals [5], a is proportional to the surface tension between the two phases [18] and is typically a length of order $0.1-0.01$ μm. An interesting discussion about this model can be found in De-Gennes [19].

B. Chemical potential and constitutive relation

Below a certain critical temperature T_c, corresponding to values $\Psi \geqslant 2$, the molar free energy given by Eqs. (2) and (3) is a double-well potential, and therefore a first-order phase transition will take place. Now, it is well known that the molar free energy can be written as [15]

$$g_{\rm eq}/RT=\mu_A x_A+\mu_B x_B, \tag{5}$$

where μ_A and μ_B denote the chemical potential of species A and B in solution, respectively, i.e.,

$$\mu_A=\frac{1}{RT}\frac{\partial(cg_{\rm eq})}{\partial c_A}, \quad \mu_B=\frac{1}{RT}\frac{\partial(cg_{\rm eq})}{\partial c_B}.$$

Here c_A and c_B denote the mole densities, that is, the number of moles per unit volume, of species A and B, respectively, and $c=c_A+c_B$ is the total mole density. Clearly, $x_A=c_A/c$ and $x_B=c_B/c$. From here we see that the two quantities $\phi=x_A$ and $(\mu_A-\mu_B)$ are thermodynamically conjugated, that is, $(\mu_A-\mu_B)=d(g/RT)/d\phi$. This result can be extended [4] defining the generalized chemical potential μ,

$$\mu=\frac{\delta(g/RT)}{\delta\phi}=\frac{\partial(g/RT)}{\partial\phi}-\boldsymbol{\nabla}\cdot\frac{\partial(g/RT)}{\partial(\boldsymbol{\nabla}\phi)}, \tag{6}$$

and substituting Eqs. (1)–(3) into Eq. (6) we obtain

$$\mu=\mu_0+\ln\frac{\phi}{1-\phi}+\Psi(1-2\phi)-a^2\nabla^2\phi, \tag{7}$$

where $\mu_0=(g_B-g_A)/RT$.

The mole densities c_A and c_B satisfy the continuity equations,

$$\frac{\partial c_A}{\partial t}+\boldsymbol{\nabla}\cdot J_A=0, \tag{8}$$

$$\frac{\partial c_B}{\partial t}+\boldsymbol{\nabla}\cdot J_B=0, \tag{9}$$

where the fluxes $\mathbf{J}_A=c_A\mathbf{v}_A$ and $\mathbf{J}_B=c_B\mathbf{v}_B$ are the local rates at which moles of species A and B pass through a unit cross section, with velocities $\mathbf{v}_A$ and $\mathbf{v}_B$, respectively. Summing Eqs. (8) and (9) we obtain the continuity equation for the total mole density,

$$\frac{\partial c}{\partial t}+\boldsymbol{\nabla}\cdot c\mathbf{v}^*=\mathbf{0}, \tag{10}$$

where

$$\mathbf{v}^*=x_A\mathbf{v}_A+x_B\mathbf{v}_B \tag{11}$$

is the mole average velocity.

Now we introduce the last assumption: the two species have the same density, so that mole- and density-based quantities are proportional to each other. Consequently, as there is no net convective flux, the average velocity $\mathbf{v}^*$ is zero, so that Eq. (10) shows that the total mole density c is constant. In addition, considering that $c_A=cx_A$, substituting Eq. (10) into Eq. (8) we obtain

$$c\frac{\partial x_A}{\partial t}+\boldsymbol{\nabla}\cdot\mathbf{J}=0, \tag{12}$$

where $\mathbf{J}$ is the diffusive flux, which is defined as follows:

$$\mathbf{J}=cx_A x_B(\mathbf{v}_A-\mathbf{v}_B). \tag{13}$$

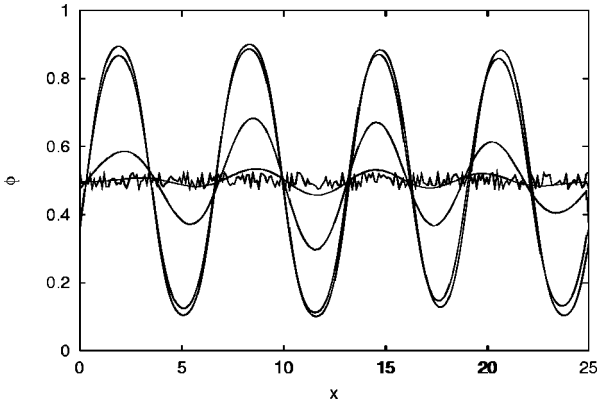

FIG. 1. Composition as a function of position for a critical instantaneous quench $\Psi=3$ at different times, when a random perturbation with amplitude $\delta\phi=0.025$ is superimposed to the initial composition $\phi=0.5$. The space and time coordinates, x and t, are scaled in terms of a and a^2/D, respectively. The curves correspond, respectively, to times $t=0$, 0.5, 1.0, 1.5, and 2.5.

The constitutive relation for **J** cannot be determined from first principles and has to be based on some reasonable assumptions. Now, the velocities of the single species, $\mathbf{v}_A$ and $\mathbf{v}_B$, are the sums of a convective part, $\mathbf{v}^*$ (which is zero, in our case), and a diffusive part, which in turn must satisfy the Gibbs-Duhem relation identically,

$$x_A\boldsymbol{\nabla}\mu_A+x_B\boldsymbol{\nabla}\mu_B=\mathbf{0}. \tag{14}$$

Therefore, comparing Eqs. (14) and (11), we conclude that it is reasonable to assume

$$\mathbf{v}_A=\mathbf{v}^*-D\boldsymbol{\nabla}\mu_A, \tag{15}$$

$$\mathbf{v}_B=\mathbf{v}^*-D\boldsymbol{\nabla}\mu_B, \tag{16}$$

where D is a composition-independent diffusion coefficient. Consequently, the expression for **J** becomes

$$\mathbf{J}=-cDx_Ax_B\boldsymbol{\nabla}\mu. \tag{17}$$

Finally, considering Eq. (7), we find that the diffusive flux can be expressed as a function of ϕ (where $\phi\equiv x_A$) only:

$$\frac{\mathbf{J}}{c}=-D\boldsymbol{\nabla}\phi+D\phi(1-\phi)[a^2\boldsymbol{\nabla}\nabla^2\phi+2\Psi\boldsymbol{\nabla}\phi +(2\phi-1)\boldsymbol{\nabla}\Psi], \tag{18}$$

which coincides with the expression for **J** used in [12]. The term $D\boldsymbol{\nabla}\phi$ in Eq. (18) represents the regular diffusion flux, while the last term vanishes for small concentrations of either solvents ($\phi\to0$ or $\phi\to1$) and for ideal mixtures ($a=\Psi=0$). Note that the a^2 term is always stabilizing and is relevant only at small length scales, while Ψ is a known function of the temperature, and near the critical temperature $T_{\rm cr}$ it is proportional to $(T_{\rm cr}-T)$.

C. Dynamical model and scaling

Substituting Eq. (18) into Eq. (12), we obtain the following governing equation:

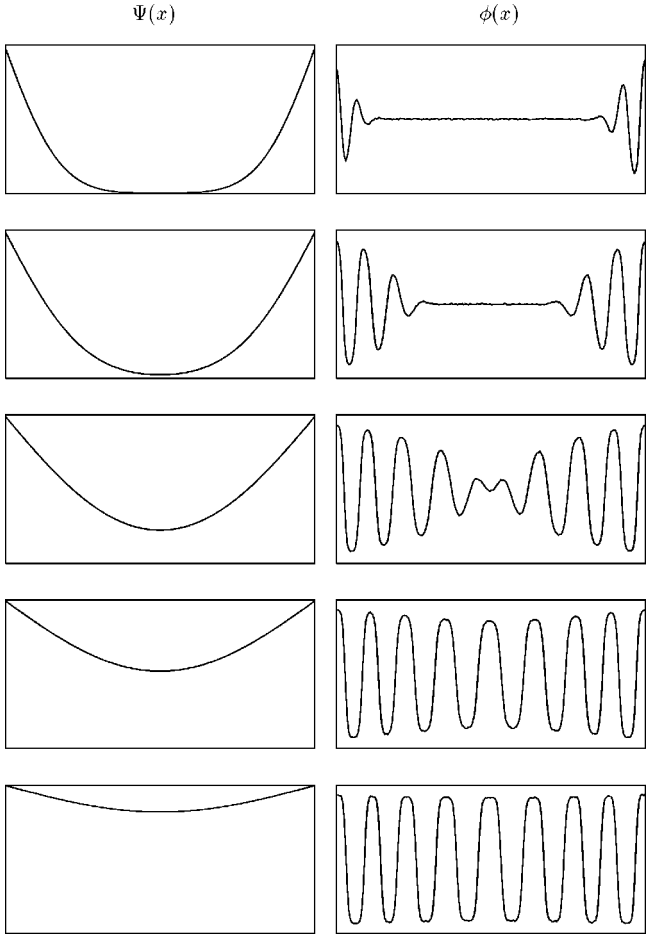

FIG. 2. Quenching depth, Ψ, and composition, ϕ, as functions of position at different times for heat diffusivity $\alpha=D$. The curves correspond to times $t=100$, 200, 500, 1000, and 2000 (given in a^2/D units). The spatial coordinate varies between 0 and $100a$, composition varies between 0 and 1, while the quenching depth solves the heat equation with $\Psi_i=2$ and $\Psi_w=3$.

$$\frac{\partial\phi}{\partial t}+D\boldsymbol{\nabla}\cdot\{-\boldsymbol{\nabla}\phi+\phi(1-\phi)[a^2\boldsymbol{\nabla}\nabla^2\phi+\boldsymbol{\nabla}(\Psi(2\phi-1))]\} +\boldsymbol{\nabla}\cdot\mathbf{j}=\mathbf{0}, \tag{19}$$

where **j** is the contribution to the material flux due to thermal fluctuations, which satisfies the fluctuation-dissipation theorem [20],

$$\langle\mathbf{j}(\mathbf{r},t)\rangle=\mathbf{0},$$

$$\langle\mathbf{j}(\mathbf{r},t)\mathbf{j}(\mathbf{r}',t')\rangle=-\frac{2}{n}D\mathbf{I}\phi(1-\phi)\,\delta(\mathbf{r}-\mathbf{r}')\,\delta(t-t'),$$

with the brackets indicating ensemble average and n denoting the number density, that is, the number of particles per unit volume. Trivially, if we also assume that the temperature quench is instantaneous, so that the temperature is uniform within the system and Ψ is constant, this equation reduces to the one considered in [12].

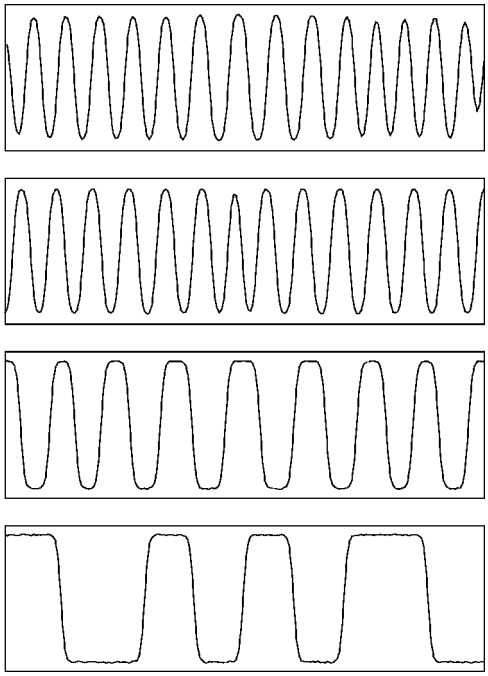

FIG. 3. Steady-state composition as a function of position for different values of the heat diffusivity, $\alpha=\infty$ (i.e., instant quenching), $10D$, $1D$, and $0.1D$, respectively. The spatial coordinate varies between 0 and $100a$, while composition varies between 0 and 1.

Since the only mechanism of mass transport that is considered here is diffusion, the length scale of the process is the microscopic length a, so that we can introduce the following scaling:

$$\tilde{\mathbf{r}}=\frac{\mathbf{r}}{a}, \quad \tilde{t}=\frac{D}{a^2}t.$$

Therefore, the continuity equation becomes

$$\frac{\partial\phi}{\partial\tilde{t}}+\tilde{\nabla}\cdot\tilde{\mathbf{J}}=0, \tag{20}$$

where

$$\tilde{\mathbf{J}}=-\tilde{\nabla}\phi+\phi(1-\phi)\tilde{\nabla}[\tilde{\nabla}^2\phi+\Psi(2\phi-1)]+\tilde{\mathbf{j}}, \tag{21}$$

with

$$\langle\tilde{\mathbf{j}}(\tilde{\mathbf{r}},\tilde{t})\rangle=\mathbf{0};$$

$$\langle\tilde{\mathbf{j}}(\tilde{\mathbf{r}},\tilde{t})\tilde{\mathbf{j}}(\tilde{\mathbf{r}}',\tilde{t}')\rangle=-2\varepsilon^2\mathbf{I}\phi(1-\phi)\,\delta(\mathbf{r}-\mathbf{r}')\,\delta(t-t'), \tag{22}$$

with $\varepsilon=(na^3)^{-1/2}$. Many recent articles have used the scaling first proposed by Grant *et al.* [21], where space is scaled through the wavelength corresponding to the fastest growing mode of the linear regime. Near the critical point, this length is much larger than a, and in our case it equals $a/\sqrt{\Psi-2}$ [see Eq. (23)]. However, for deep quenches, the $\sqrt{\Psi-2}$ factor is an $O(1)$ quantity, and can therefore be omitted. In addition, in the slow quench case, which we consider here, where Ψ is a function of T, this scaling would introduce additional terms in the governing equation, unnecessarily complicating the analysis.

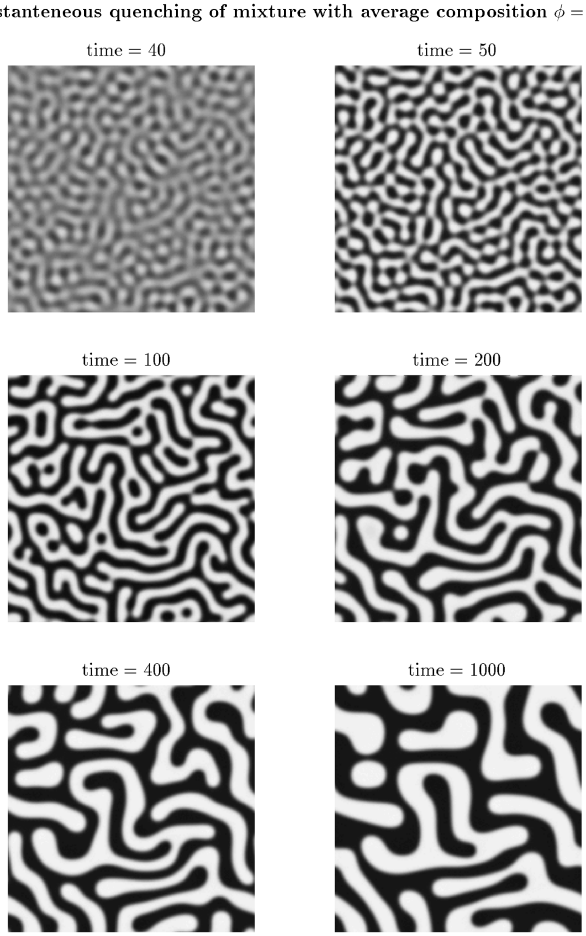

FIG. 4. Composition as a function of position for a critical instantaneous quench $\Psi=3$ at different times. The size of the system is $100a\times100a$, with periodic boundary conditions. Snapshots correspond, respectively, to times $t=20$, 60, 100, 500, 1000, and 2000, expressed in a^2/D units. The gray level varies linearly between black and white, corresponding to concentrations $\phi=\phi^A_{\rm eq}$, and $\phi=\phi^B_{\rm eq}$, respectively.

III. NUMERICAL RESULTS

We solved Eq. (20) using an explicit finite difference method on a uniform $N\times M$ two–dimensional grid with spacing $[(i\Delta x,j\Delta y),i=1,N,\ j=1,M]$ and time discretization $[n\Delta t,n=1,2,\ldots]$, with $\Delta x/a,\Delta y/a\approx0.5-2$, and $\Delta t/(a^2/D)\approx0.1$–$0.001$. We adopted a cell-centered representation for the concentration variable $\phi^n_{ij}(t)$, and discretized the right-hand side of Eq. (20) in flux conservation form, using a second-order accurate approximation of the spatial derivatives. The equations are advanced in time, using a straightforward explicit Eulerian step, and we chose the time step Δt in such a way to satisfy the CFL stability condition for the discretized equations. This way, the numerical scheme is $O(\Delta x^2,\Delta t)$ accurate. The background noise was simulated generating a random concentration field of amplitude,

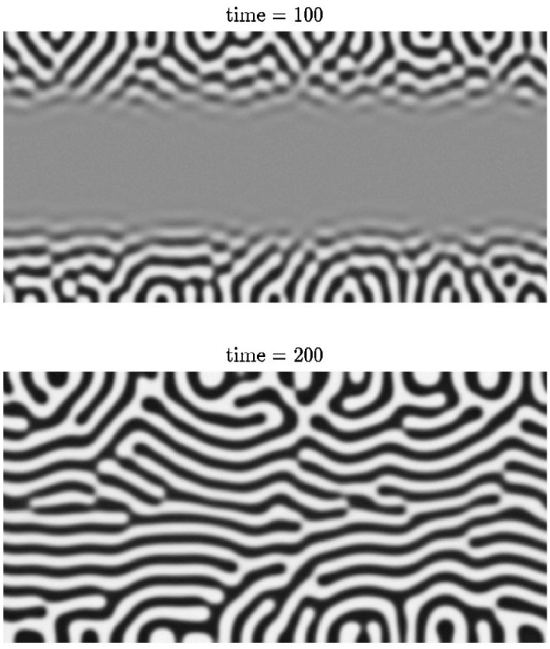

FIG. 5. Composition as a function of position at different times after the temperature of the upper and lower walls has been quenched from $\Psi_i=2$ to $\Psi_w=3$, with heat diffusivity $\alpha=10D$. The size of the system is $200a\times100a$, with periodic boundary conditions in the horizontal direction, and no-flux boundary conditions in the vertical direction, to simulate a long, horizontal tube. Snapshots correspond, respectively, to times $t=100$, 200, and 400, expressed in a^2/D units. The gray level varies linearly between black and white, corresponding to a concentrations $\phi=\phi^A_{\rm eq}$, and $\phi=\phi^B_{\rm eq}$, respectively.

$$\delta\phi=\frac{\varepsilon}{(\Delta x/a)(\Delta tD/a^2)}\approx 0.1\text{–}0.01,$$

which was uncorrelated both in space and in time, so as to satisfy Eq. (22). That means that at each time step a spatially uncorrelated noise was added to the concentration field, and was then subtracted at the next time step, only to be replaced with another spatially uncorrelated background noise of the same amplitude.

In the following, we present results corresponding to temperature quenches where the Margules parameter Ψ increased from $\Psi_i=2$ (which is its critical value) to $\Psi_w=3$. Similar results were obtained when we performed simulations with $\Psi_w=2.1$ and 2.3. Two cases were considered, with uniform initial concentration field $\phi_0=0.5$, corresponding to a critical quench, and $\phi_0=0.4$ (off-critical quench).

A. One-dimensional case

First, we validated our numerical scheme by solving the one-dimensional version of Eq. (20) with periodic boundary conditions, considering an instantaneous, critical, and uniform quench with $\Psi=3$ and $\phi_0=0.5$. As we mentioned above, in this case our equation and boundary conditions become essentially the same as those used in [12], the only difference being that the initial conditions and the numerical technique employed here are different. (Mauri *et al.* [12] solved the problem for periodic and pulsed initial conditions, using a split-step method in time and a pseudospectral collocation method in space.) As we can see in Fig. 1, identical results were obtained, as initial, exponentially growing instabilities are later saturated by the effect of the nonlinear terms. Eventually, the concentration distribution tends to a steady, periodic profile, with a period and an amplitude which correspond to the fastest growing mode of the linear regime, i.e.,

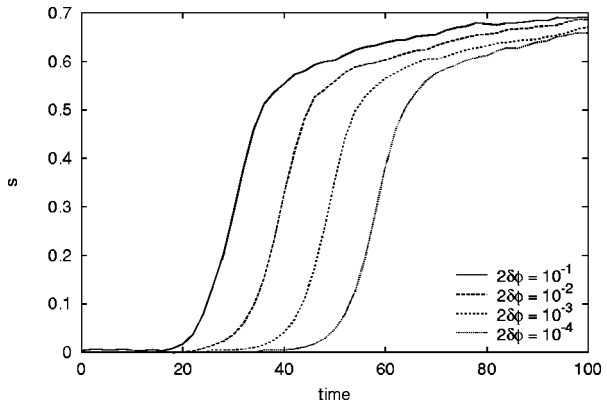

FIG. 6. Separation depth, s, as a function of time for a critical instantaneous quench $\Psi=3$ and different amplitudes of the background noise, $\delta\phi=0.5\times10^{-1}$, 0.5×10^{-2}, 0.5×10^{-3}, and 0.5×10^{-4}, with time expressed in terms of a^2/D.

$$\lambda_0=\frac{2\pi a}{\sqrt{\Psi-2}}. \tag{23}$$

Qualitatively, the relaxation time that is needed to reach steady state also agrees with that obtained in [12], i.e., $\tau_0=\lambda_0^2/D$.

Our next step was to study a critical quench where temperature, and therefore Ψ, is a known function of position and time. Since near the critical point we have $\Psi\propto(T-T_{\rm cr})$, then $\Psi(x,t)$, with $0\leqslant x\leqslant L$, can be obtained from the heat conduction equation, $\partial\Psi/\partial t=\alpha\partial^2\Psi/\partial x^2$, with initial and boundary conditions, $\Psi(x,0)=\Psi_i$ and $\Psi(0,t)=\Psi(L,t)=\Psi_w$, describing heat propagation from the walls of the container towards the center. Typical solutions for $\phi(x,t)$, together with the corresponding $\Psi(x,t)$, are given in Fig. 2, where no-flux boundary conditions have been applied. From the sequence of plots in Fig. 2 it is easy to see that the instability propagates from the edges towards the center of the cell, growing without changing its length scale until the equilibrium state is reached. As shown in Fig. 3, the steady-state concentration distribution appears to be periodic across the domain, provided, naturally, that the cell size L is either much larger than, or an exact multiple of, the droplet size; if none of these conditions is satisfied, the periodic steady-state solution can never be reached, as it is evident from the concentration profile at the bottom of Fig. 3. The period of the steady-state solutions decreases as the thermal diffusivity α increases, until, when $\alpha>D$, it becomes equal to the period λ_0 obtained for instant quenching, with $\alpha\to\infty$. Clearly, since in most cases we have $\alpha\gg D$, this result shows that the assumption of instant quenching is very reasonable. Our results can be considered an extension of those obtained by Carmesin *et al.* [22], who studied the influence

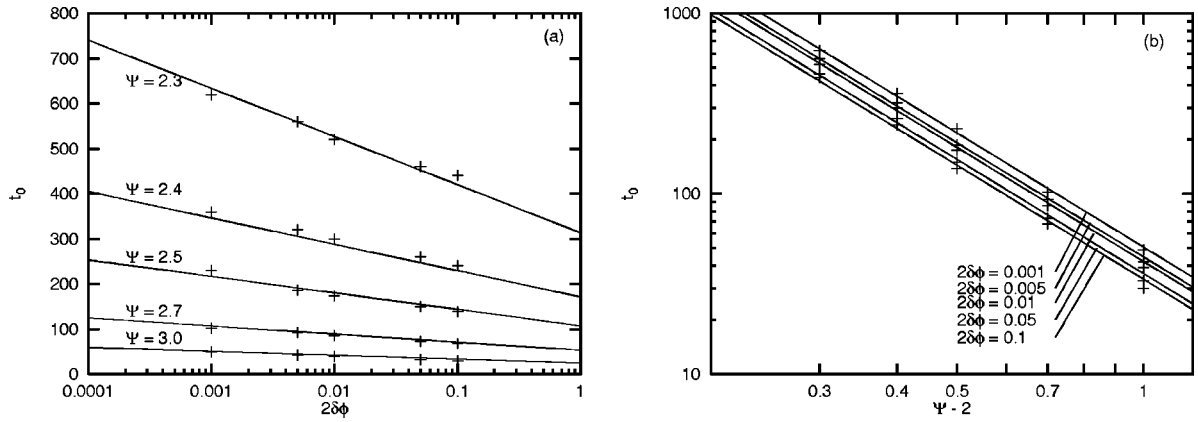

FIG. 7. Initial time t_0 as a function of the background noise $\delta\phi$ (a) and the quenching depth $(\Psi-2)$ (b). Points refer to the results of numerical simulations with $\phi_0=0.5$, while the continuous line represents the correlation $t_0=(A-B\ln\delta\phi)/(\Psi-2)^c$, with $A=22.5$, $B=3.7$, and $c=2.1$.

of a continuous quenching on the initial stages of spinodal decomposition by using the linearized theory of spinodal decomposition.

B. Two-dimensional case

First, Eq. (20) was solved for an instantaneous, critical quench, with periodic boundary conditions. Our simulations showed that at first the system tends to form circular drops whose size, λ_0, equals that of the one-dimensional domains. However, unlike the one-dimensional case, this is not the steady-state solution (see Fig. 4), as the system rapidly evolves towards the formation of single-phase microdomains separated by sharp interfaces, which then merge to form filaments. This bicontinuous infinite-cluster morphology has been observed experimentally in binary fluid mixtures by Cumming *et al.* [23], and has been numerically simulated, among others, by Rogers, Elder, and Desai [13] and by Farrell and Valls [24]. Our simulations show that this dendroid-like structure continues to deform, increasing its thickness, and, above all, further reducing the total area of the interface. So, for example, microdomains of one phase entirely surrounded by the other phase evolve towards assuming a spherical shape. However, contrary to the behavior of the mixtures of totally immiscible liquids, these small, isolated drops continue to deflate even after they become spherical, until they diffuse out completely (see the evolution of the drop located in the lower left part of Fig. 4).

As expected, a different morphology is obtained for nonisotropic systems. For example, in Fig. 5 we show the concentration distribution in a system with periodic boundary conditions in the horizontal direction, and no-flux boundary conditions at the walls in the vertical direction, thereby simulating the behavior of a long horizontal tube. As the walls of the tube are quenched, the temperature of the whole system changes in time towards its steady state. As expected, the morphology of the system is composed of ''serpentines'' with a well specified horizontal preferential direction, forming typical striped pattern as in Sagui and Desai [25]. As in the one-dimensional case, the thickness of these stripes increases as the heat conductivity of the system decreases.

As a quantitative characterization of the decomposing system, we define the separation depth s, measuring the ''distance'' of the single-phase domains from their equilibrium state, i.e.,

$$s=\left\langle \frac{\phi(\mathbf{r})-\phi_0}{\phi_{\mathrm{eq}}(\mathbf{r})-\phi_0}\right\rangle, \tag{24}$$

where ϕ_0 is the initial composition and the angular brackets indicate volume average. Here ϕ_{eq} is the steady-state composition of the the A-rich phase, ϕ_{eq}^A, or the B-rich phase, ϕ_{eq}^B, depending on the local composition $\phi(\mathbf{r})$,

$$\phi_{\mathrm{eq}}(\mathbf{r})=\phi_{\mathrm{eq}}^A, \quad \phi(\mathbf{r})>\phi_0,$$

$$\phi_{\mathrm{eq}}(\mathbf{r})=\phi_{\mathrm{eq}}^B, \quad \phi(\mathbf{r})<\phi_0.$$

For $\Psi=3$, the equilibrium compositions are $\phi_{\mathrm{eq}}^A=0.92$ and $\phi_{\mathrm{eq}}^B=0.08$. In Fig. 6 the separation depth s is plotted as a function of time, showing that the phase separation process can be divided into three stages. During the first stage, $t<t_0$, the concentration ϕ remains approximately constant, i.e., there is no phase separation; then, for $t_0<t<t_1$, the concentration changes rapidly, with the exact values of t_0 and t_1 defined such that this rate of change is larger than a given critical value; finally, during the third stage, $t>t_1$, the separation depth s increases much more slowly. As shown in Fig. 7, the value of t_0 depends on the depth of the temperature quench, $(\Psi-2)$, and the amount of the random noise, $\delta\phi$, through the correlation $t_0=(A-B\ln\delta\phi)/(\Psi-2)^c$, where A, B, and c are constants that depend on the value of ϕ_0. In the second stage, the time interval (t_1-t_0) appears to be independent of the random noise (see Fig. 7), and is approximately equal to the relaxation time $\tau_0=\lambda_0^2/D$. Finally, during the last stage, $t>t_1$, the separation depth s continues to change, although more gradually, tending asymptotically to 1, indicating that, although the system is composed of single-phase domains separated by sharp interfaces, the composition inside these domains is not equal to its final equilibrium value. The same conclusion was reached even when all points adjacent to the interfaces were removed; for example, when the regions with $|\phi(\mathbf{r})-\phi_0|<0.1$ were not included in the definition (24) of the separation depth, the resulting curves differed from those in Fig. 6 by 3% or less. There-

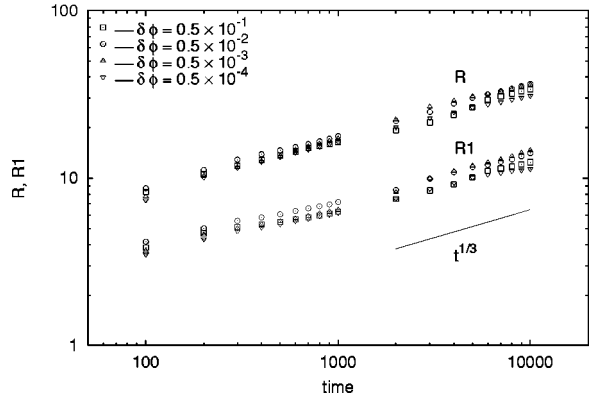

FIG. 8. Characteristic size of the microdomains, R, defined through Eq. (25) and expressed in a units, as a function of time, t, expressed in a^2/D units, after an instantaneous critical quench $\Psi=3$. The length scale R is compared to $R1$, representing the characteristic size of the microdomains as defined by Desai *et al.* [13]. The continuous line represents the correlation $R=10t^{1/3}$.

fore, the local equilibrium assumption, stating that no change in composition occurs after the formation of sharp interfaces, is not valid, which implies that most of the scaling concepts should be revised. Although an identical conclusion was reached by Tanaka and Araki [26] in the case of fluid systems, this is the first time to our knowledge that a strong violation of local equilibrium has been observed for spinodal decomposition under small, or zero, fluidity conditions.

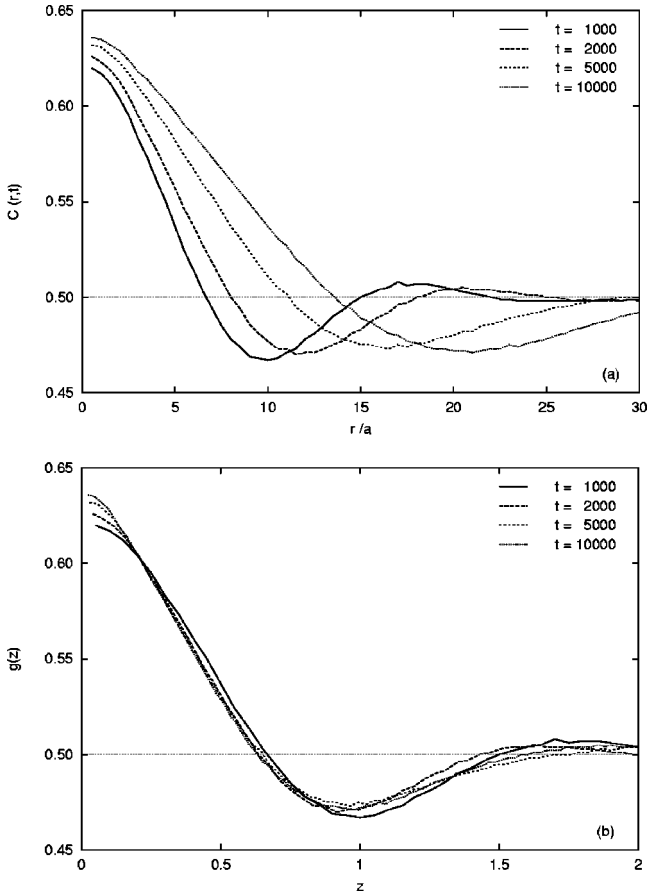

FIG. 9. Radial pair correlation function, $C(r,t)$, after an instantaneous critical quench $\Psi=3$, as a function of r for different t (a) and as a function of the self-similar parameter $z=r(aDt)^{-1/3}$ (b).

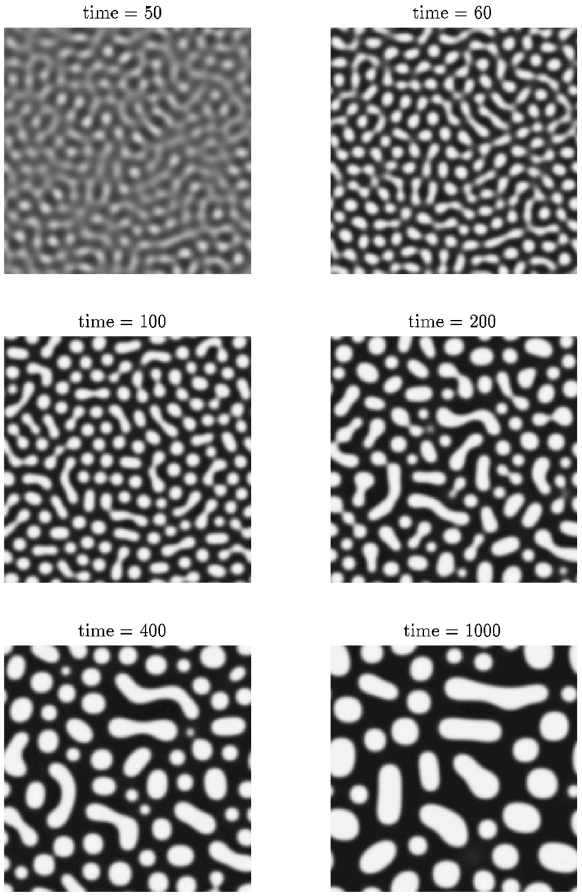

FIG. 10. Composition as a function of position for $\Psi=3$ at different times after an instantaneous off-critical quench with $\phi_0=0.4$. The size of the system is $100a\times100a$, with periodic boundary conditions. Snapshots correspond, respectively, to times $t=20$, 60, 100, 500, 1000, and 2000, expressed in a^2/D units. The gray level varies linearly between black and white, corresponding to a concentrations $\phi=\phi^A_{\rm eq}$ and $\phi=\phi^B_{\rm eq}$, respectively.

During the last stage of the separation process, the characteristic size of the microdomains appears to be independent of the depth of the temperature quench and of the background noise and, as shown in Fig. 8, it grows according to the $\frac{1}{3}$ law predicted by Lifshitz and Slyozov [10]. In Fig. 8 we have plotted the characteristic length,

$$R(t)=a\frac{\sum\,(\phi_k(t)/k)}{\sum\,\phi_k}, \tag{25}$$

where $\phi_k(t)$ is the Fourier transform of the concentration distribution field $\phi(\mathbf{r},t)$, showing that $R(t)\propto(aDt)^{1/3}$. These results are in agreement with those of Desai *et al.* [13], who have defined the typical size R_1 as the first zero of the radial pair correlation function $C(r,t)-\phi_0$, where

$$C(r,t)=\sqrt{\frac{1}{2\pi}\int_0^{2\pi}\langle\phi(\mathbf{r}'+\mathbf{r},t)\phi(\mathbf{r}',t)\rangle d\theta},\quad \mathbf{r}=(r,\theta). \tag{26}$$

In Fig. 9, $C(r,t)$ is plotted as a function of r for different t, showing that the different curves collapse into a self-similar solution, $g(z)$, with $z=r(aDt)^{-1/3}$.

We have also studied the phase separation due to an off-critical quench, in which $\phi_0=0.4$, i.e., in which there is more A than B. As expected, instead of interconnected domains, we observe the formation of isolated drops of the B-rich phase immersed in one large domain of the A-rich phase (see Fig. 10), in agreement with some previous theoretical [24,27,13] and experimental [23] findings, and consistent with the experimental evidence [28] that stable emulsions tend to form when a liquid mixture is quenched within the metastable region of its phase diagram.

IV. CONCLUSIONS

In this work we have studied the spinodal decomposition in a binary mixture in which the diffusion coefficient (mobility) depends on the local composition field ϕ, using an expression for the free energy of the system which includes its ideal (i.e., entropic) part and its nonideal counterpart (using Margules expression), instead of the simpler ϕ^4 form of the Cahn-Hilliard-Cook model and of the Landau theory of phase transition.

We have shown that a one-dimensional system will reach a steady state, consisting of a periodic concentration profile independent of the initial perturbation. For instantaneous quenches, the period of the steady-state solution is equal to the fastest growing mode, in agreement with previous results [12], while for slow quenches this period increases. This last result is new.

In two dimensions, although at first the system will reach a similarly periodic concentration profile, then it continues to evolve towards a stringlike morphology, trying to minimize the area of the interface between the two phases. This dendroidlike structure continues to deform, increasing its thickness, and, above all, further reducing the total area of the interface. In particular, during the late stage of the process, the domains coarsen as a 1/3 power of time. Similar results are obtained both for critical and off-critical quenches.

Our results were compared with those obtained by Rogers, Elder, and Desai [13], who studied spinodal decomposition using the Cahn-Hilliard-Cook model both at early and late times, and for critical as well as off-critical quenches. Since the Cahn-Hilliard-Cook expression of the free-energy density is an expansion of the expression that we have used, it is not surprising that during the early stages of the process our results were in perfect agreement with [13]. During the last stage of the process, we found that the morphology of the system was also remarkably similar to that obtained by [13], apparently indicating that this result is independent of the expression of the free energy that has been used in the simulation. The influence of the physical model, instead, appears to greatly influence the composition field within and without the microdomains, which, as evidenced in the plot of the separation depth s of Fig. 6, is not homogeneous and changes with time. The violation of the commonly accepted assumption of local equilibrium, stating that no change in composition occurs after the formation of sharp interfaces, is perhaps the main contribution of this work, indicating that although the general behavior of phase separating systems (i.e., their morphology) is self-similar and model-independent, the same is not true for the separation depth.

ACKNOWLEDGMENTS

During this work, N.V. and R.M. were supported in part by the National Science Foundation under Grant No. CTS-9634324.

[1] P. DeBenedetti, *Metastable Liquid Concepts and Principles* (Princeton University Press, Princeton, NJ, 1996), Chap. 3.

[2] J. Frenkel, *Kinetic Theory of Liquids* (Dover, New York, 1946).

[3] Reviews on spinodal decomposition can be found in P.C. Hohenberg and B.I. Halperin, Rev. Mod. Phys. **49**, 435 (1977); J.S. Langer, in *Systems Far from Equilibrium*, edited by L. Garrido, Lecture Notes on Physics No. 132 (Springer Verlag, Berlin, 1980); J.D. Gunton, M. San Miguel, and P.S. Sahni, in *Phase Transition and Critical Phenomena*, edited by C. Domb and J.L. Lebowitz (Academic Press, London, 1983), Vol. 8.

[4] J.W. Cahn and J.E. Hilliard, J. Chem. Phys. **28**, 258 (1958); **31**, 688 (1959); J.W. Cahn, *ibid.* **30**, 1121 (1959); Acta Metall. **9**, 795 (1961).

[5] J.D. van der Waals, Z. Phys. Chem., Stoechiom. Verwandtschaftsl. **13**, 657 (1894); reprinted in J. Stat. Phys. **20**, 200 (1979).

[6] J.W. Cahn, Acta Metall. **14**, 1685 (1966); Trans. Metall. Soc. AIME **242**, 166 (1968).

[7] S.W. Koch, R.C. Desai, and F.F. Abraham, Phys. Rev. A **26**, 1015 (1982).

[8] See, for example, G.F. Mazenko and R.A. Wiskham, Phys. Rev. E **51**, 2886 (1995); A. Nakahara, T. Kawakatsu, and K. Kawasaki, J. Chem. Phys. **99**, 9853 (1993); N. Akaiwa and P.W. Voorhees, Phys. Rev. E **49**, 3860 (1994); A. Chakrabarti, R. Toral, and J.D. Gunton, *ibid.* **47**, 3025 (1993).

[9] K. Binder, Phys. Rev. A **29**, 341 (1984); Physica A **140**, 35 (1986); W. Klein and C. Unger, Phys. Rev. B **28**, 445 (1983); C. Unger and W. Klein, *ibid.* **29**, 2698 (1984).

[10] I.M. Lifshitz and V.V. Slyosov, J. Phys. Chem. Solids **19**, 35 (1961); C. Wagner, Z. Elektrochem. **65**, 581 (1961); E.D. Siggia, Phys. Rev. A **20**, 595 (1979); G.F. Mazenko, Phys. Rev. E **50**, 3485 (1994), and reference therein.

[11] W.R. White and P. Wiltzius, Phys. Rev. Lett. **75**, 3012 (1996).

[12] R. Mauri, R. Shinnar, and G. Triantafyllou, Phys. Rev. E **53**, 2613 (1996).

[13] T.M. Rogers, K.R. Elder, and R.C. Desai, Phys. Rev. B **37**, 9638 (1988); K.R. Elder, T.M. Rogers, and R.C. Desai, *ibid.* **38**, 4725 (1988); T.M. Rogers and R.C. Desai, *ibid.* **39**, 11 956 (1989); K.R. Elder and R.C. Desai, *ibid.* **40**, 243 (1989).

[14] P.C. Hohenberg and B.I. Halperin, Rev. Mod. Phys. **49**, 435 (1977).

[15] J.M. Prausnitz, R.N. Lichtenthaler, and E. Gomes de Azevedo, *Molecular Thermodynamics of Fluid-Phase Equilibria*, 2nd ed.

(Prentice-Hall, New York, 1986).

[16] E.A. Guggenheim, *Mixtures* (Oxford University Press, Oxford, 1952).

[17] J.H. Hildebrand and S.E. Wood, J. Chem. Phys. **1**, 817 (1933).

[18] The characteristic length a is given by the following expression:

$$a=\frac{1}{2\sqrt{\Psi-2}(\Delta\phi)_{\mathrm{eq}}^{2}}\frac{\sigma M_{W}}{\rho RT},$$

where σ and $(\Delta\phi)_{\mathrm{eq}}$ are the surface tension and the composition difference between the two phases at equilibrium, while M_W and ρ are their molecular weight and density, respectively (here we assume that A and B have the same physical properties).

[19] P.G. deGennes, J. Chem. Phys. **72**, 4756 (1980).

[20] L. Landau and L. Lifshitz, *Fluid Mechanics* (Pergamon, New York, 1953).

[21] M. Grant, M. San Miguel, J. Viñals, and J.D. Gunton, Phys. Rev. B **31**, 3027 (1985).

[22] H.-O. Carmesin, D.W. Heermann, and K. Binder, Z. Phys. B **65**, 89 (1986).

[23] A. Cumming, P. Wiltzius, F.S. Bates, and J.H. Rosedale, Phys. Rev. A **45**, 885 (1992).

[24] J. E. Farrell and O.T. Valls, Phys. Rev. B **40**, 7027 (1989); **42**, 2353 (1990); **43**, 630 (1991).

[25] C. Sagui and R.C. Desai, Phys. Rev. E **49**, 2225 (1994).

[26] H. Tanaka and T. Araki, Phys. Rev. Lett. **81**, 389 (1998).

[27] R. Toral, A. Chakrabarti, and J.D. Gunton, Phys. Rev. B **39**, 901 (1989).

[28] R. Gupta, R. Mauri, and R. Shinnar, Ind. Eng. Chem. Res. **35**, 2360 (1996).